

# The impact of transmission power levels set size on lifetime of wireless sensor networks in smart grids

Hüseyin Uğur YILDIZ<sup>1\*</sup>

<sup>1</sup> Department of Electrical and Electronics Engineering, Faculty of Engineering, TED University, Ankara, Turkey

---

Received: .201

• Accepted/Published Online: .201

• Final Version: .201

---

**Abstract:** Wireless Sensor Networks (WSNs) have been confirmed as one of the most promising technologies for many smart grid (SG) applications due to their low complex nature and inexpensive costs. A typical WSN is formed with numerous battery limited sensor nodes mounted on critical components of a SG system for monitoring applications. Acquired monitoring data by sensor nodes are conveyed to the base station generally by using multi-hop communication techniques. WSN based SG applications encounter severe propagation losses due to extreme channel conditions of the SG environment. In order to reduce possible packet errors caused by channel variations, transmission power control approaches can be adopted where the set size of available transmission power levels differs among the utilized hardware platforms. Usage of low transmission power levels can reduce the energy dissipation of nodes which may lead high packet drops. On the other hand, usage of high transmission power levels can prevent packet errors. Nonetheless, this alternative solution may lead premature death of sensor nodes. Depending on the networking conditions, it is possible to confront applications such that the utilization of all available power levels provided by the node hardware may be unnecessary. In order to overcome this issue, determination of optimal transmission power levels set size for WSN based SG applications becomes a critical research topic to prolong the network lifetime. In this work, we propose an optimization model to maximize the network lifetime with limiting the size of the transmission power levels set. Furthermore, we propose two strategies which are built on top of the optimization model to investigate the impact of most used and optimal power levels on WSN lifetime considering several SG environments under various networking conditions.

**Key words:** smart grids, wireless sensor networks, optimization, network lifetime, power levels set size

## 1. Introduction

For many years, power grid systems were monitored and maintained through expensive wired communication principles [1]. In recent years, power grid systems are diagnosed by using wireless communication techniques in order to reduce high expenditure costs of wired communications [2, 3]. One of the most suitable wireless communication technologies used in power distribution systems is called Wireless Sensor Networks (WSNs). WSNs are constructed with numerous battery limited inexpensive sensor nodes and a base station where the acquired data by sensor nodes are transmitted to the base station either by using single-hop or commonly multi-hop communication techniques. Usage of modern communication technologies (such as WSNs) in traditional power grid systems for monitoring, automation, and control purposes creates the paradigm of *smart grids* (SGs) [4]. Limited battery power of sensor nodes poses a great challenge for long term monitoring in SG applications.

---

\*Correspondence: hugur.yildiz@tedu.edu.tr

WSN based SG systems are subject to severe propagation losses due to the electromagnetic interference generated in the SG infrastructure [5, 6]. In order to reduce packet errors due to severe propagation losses, transmission power control (TPC) approaches can be adopted. The idea behind TPC approaches is to adjust the transmission power levels from a set of available discrete transmission power levels [7] for achieving a reliable communications performance. TPC techniques can be categorized as network-level (i.e., a global transmission power level is employed throughout the network) and link-level (i.e., each link can adjust their transmission power level locally) [8].

The size (cardinality) of the transmission power levels set depends on the WSN node hardware used in SG systems. One of the most popular WSN node platforms used in SG systems is the Tmote Sky platform [9]<sup>1</sup>. This node hardware uses Chipcon CC2420 radio module which has 31 different transmission power levels. Another popular node platform is the Mica2 which uses Chipcon CC1000 radio module having 26 different transmission power levels [7]. Regardless of the node platform that is used, packet errors can be mitigated by utilizing the maximum available transmission power level. This approach has a drawback of energy efficiency such that nodes consume excessive amount of energy for transmission which would yield low lifetimes. To attain energy efficiency, less amount of energy can be consumed by the nodes if lower transmission power levels are utilized, however with this way the chance of packet drops increases. Hence, there is a trade-off of utilizing transmission power levels to attain the energy efficiency and prolong the network lifetime. On the other hand, depending on the networking area, the usage of transmission power levels may vary greatly. When the network size is small, propagation losses are tended to be lower when compared to larger network sizes. In this case, there is a tendency of using lower transmission power levels. As the network size increases, propagation losses increase which would result in usage of higher transmission power levels to avoid packet errors. In these possible scenarios, some of the available transmission power levels (depending on the node platform that is used in SG systems) may be unused. Thus, determination of optimal transmission power levels plays a vital role in lifetime elongation when designing distributed protocols for WSNs in SGs.

In this work, we develop an optimization model by using the mixed integer linear programming (MILP) framework that maximizes the network lifetime. By using this optimization model, two strategies are proposed to determine the most used and optimal transmission power levels sets for WSN based SG applications. We enumerate our original contributions as follows:

1. We develop an MILP model that maximizes the network lifetime with limiting the size of the transmission power levels set. The proposed MILP model employs a detailed handshaking based link-layer energy dissipation model which utilizes a link-level TPC approach. Moreover, the link-layer model uses the energy consumption characteristics of Tmote Sky node platforms and an experimental path loss model (i.e., log-normal shadowing) considering the path loss parameters for several SG environments described in [1].
2. We propose a strategy, which is built onto the aforementioned MILP model, called “Histogram Based Power Levels Decision (HB-PLD)” strategy that determines the most used transmission power levels for a maximized lifetime according to the transmission power level usage statistics for six SG environments considering various network sizes without limiting the size of the transmission power levels set. Furthermore, we gradually reduce the cardinality of the most used transmission power levels set and investigate the impact of this approach on the network lifetime quantitatively.

---

<sup>1</sup>Tmote Sky datasheet: [http://www.snm.ethz.ch/snmwiki/pub/uploads/Projects/tmote\\_sky\\_datasheet.pdf](http://www.snm.ethz.ch/snmwiki/pub/uploads/Projects/tmote_sky_datasheet.pdf)

- 1 3. We also propose another strategy called “Optimization Based Power Levels Decision (OB-PLD)” strategy  
2 which determines the optimal transmission power levels that maximize the network lifetime with limiting  
3 the size of the transmission power levels set.
- 4 4. We numerically compare lifetime and solution time differences between HB-PLD and OB-PLD strategies  
5 for various network densities and several SG environments.

6 The rest of the paper is organized as follows. We present the related work on the determination of  
7 optimal transmission power level sets for wireless networks and especially WSNs in Section 2. Our system  
8 model including the wireless channel model, link-layer energy consumption model, optimization framework, and  
9 proposed strategies is described in Section 3. The results of the numerical analysis are provided in Section 4.  
10 Conclusions are presented in Section 5.

## 11 2. Related Work

12 In literature, there has been a great interest on the transmission power levels selection approaches for wireless  
13 networks in the last two decades [10–19]. Moreover, there is a growing body in the literature on this research  
14 topic for WSNs. We present an overview of the related work in the following paragraphs.

15 In [10], a single channel ALOHA protocol is considered and its throughput is investigated under full-load  
16 conditions by considering both exponential back-off retransmission method and capture effects. Packets are  
17 transmitted with various power levels where the set size of power levels is in the interval 1–10. In [11], authors  
18 developed an algorithm to determine optimal set of transmission powers in each link for mobile networks  
19 which use directional antennas deployed in hostile environment. The proposed method avoids interceptions  
20 by adversaries with minimum probability. The set size of transmission power levels in each directional bin is  
21 given in the interval 1–4. In [12], an adaptive  $M$ -ary quadrature amplitude modulation (M-QAM) system is  
22 considered for throughput maximization. The proposed system uses a small number of power levels (i.e., 2 to 3)  
23 and code rates. It was shown that the proposed system can achieve high throughput as the continuous adaptive  
24 systems in slow fading environments. Another work is performed for M-QAM systems to identify optimal delay  
25 constrained rate and power adaptation for type-I hybrid automatic repeat request (ARQ) scheme over fading  
26 channels by using a Markov decision process in [13]. The proposed method uses a discrete power level in each  
27 time slot which is selected from a predetermined transmission power level set. In [14], the transmission power  
28 is modeled as a function of packet collisions and selection of power levels is investigated in large scale ALOHA  
29 networks in a decentralized manner. In that work, authors considered a finite transmission power levels set  
30 such that the transmission power level is increased with a power step (which can be either small or large) until  
31 the packet transmission within the defined interval is successful. Properly chosen larger power steps are shown  
32 to have higher throughput when compared to small power steps which yield a decline in throughput when  
33 the network load is high. In [15], an adaptive transmission power scheme for flat-fading wireless channels is  
34 developed. The proposed transmission mechanism is based on a set of finite power levels per code. Authors  
35 concluded that using 4 codes and 4 power levels per code results in an average spectral efficiency within 1 dB of  
36 the continuous-rate continuous-power Shannon capacity. In [16], a cognitive radio system is considered where  
37 the secondary users vary their transmission powers depending on the information contained in the spectrum  
38 sensor. Peak power and average interference constraints are enforced at the secondary and primary users,  
39 respectively. Authors revealed that if any transmission is occurring, only the peak power level is utilized. In  
40 [17], effects of TPC on interference for wireless mesh networks on a real testbed are investigated. Transmission

1 power levels set has a cardinality of 6 and contains power levels between 7 dBm to 19 dBm with a step size of  
 2 2 dBm. In that work, power level for each testbed is determined which avoids interference while keeping each  
 3 link's robustness. In [18], an algorithm is proposed to determine optimal power levels which minimize the total  
 4 transmission power for each retransmission period for hybrid ARQ method used in quasi-static Rayleigh fading  
 5 channels. In [19], an analytical model by using randomized transmission power for throughput maximization in  
 6 IEEE 802.11 networks is developed. The proposed solution determines the attempt probability of a randomly  
 7 selected node as well as obtaining the optimal probability mass function of transmission powers to maximize  
 8 the network throughput. In that work, only 5 transmission power levels are considered.

9 The literature on the selection of transmission power levels in WSNs is growing day-to-day [7, 20–28].  
 10 In [20], authors proposed a distributed power controlled contention based medium access control (MAC) layer  
 11 protocol for WSNs. Authors considered a radio module which has 8 distinct power levels between 0.05 mW and  
 12 25 mW. In [21], an analytical framework is proposed to evaluate the advantages of using variable transmission  
 13 power levels in WSNs for geographical routing. In that work, the set size of available transmission power  
 14 levels is defined in the interval 1–4. [22] and [23] investigated link channel characteristic in wireless body area  
 15 sensor networks. Among these works, Natarajan et al. [22] used three predetermined power level sets (i.e.,  
 16 -25 dBm, -15 dBm, and -10 dBm) for the analysis. On the other hand, Lee et al. [23] used the all available  
 17 power levels for CC2420 radios. In [24], the joint impact of packet length and transmission power level on  
 18 the energy consumption between two WSN nodes using CC1000 radios is investigated. In that work, authors  
 19 adopt 26 transmission power levels of CC1000 radios. In [25], discrete TPC and rate adaption algorithms are  
 20 proposed for ultra-reliable machine-to-machine control applications in which a finite set of transmit rates is only  
 21 supported (with cardinality 4 and 8). In [26], two topology control techniques (i.e., depth adjustment and TPC)  
 22 for geographic routing in underwater WSNs are studied. In that work, all underwater nodes are identical and  
 23 the set size of transmission power levels is 7. In [27], a discrete TPC scheme is developed for Poisson-clustered  
 24 ad hoc networks where each transmitter can use predetermined discrete transmission power levels. In [28], total  
 25 power consumption in the network is minimized while guaranteeing strong connectivity between node pairs  
 26 in the network. Sensor nodes are allowed to use only 2 power levels. In our previous work [7], we focused  
 27 on determining optimal transmission power levels set for conventional terrestrial WSNs which maximizes the  
 28 network lifetime. 26 different power levels of CC1000 radios is employed in that work. Our results revealed  
 29 that the drop in maximum network lifetime is observed at most 5% if the set size of transmission power levels  
 30 is reduced to 13 from 26.

31 As a summary, in the literature of determining the optimal transmission power levels set, some works  
 32 aimed to maximize the throughput of the network [10, 12–14, 16, 19, 27] while some others focused on the  
 33 minimization of the energy consumption in the network [18, 20, 21, 24, 26, 28]. There are also several studies  
 34 considering other important performance metrics such as link quality [17, 22, 23], concurrent transmission time  
 35 [25], average spectral density [15], and accuracy of localization [11]. Moreover, there are only a few works  
 36 that determine optimal transmission power levels set by using a real WSN node platform (such as CC1000  
 37 and CC2420) [7, 22–24]. To the best of our knowledge, there are no controlled studies that investigate the  
 38 impacts of determining transmission power levels which maximize the network lifetime by using an actual WSN  
 39 node platform quantitatively for SG applications. In order to fill this gap in the literature, in this study, we  
 40 develop an optimization model to determine the most used and optimal transmission power levels sets for WSN  
 41 based SG applications with the objective of maximization of network lifetime by using the power consumption  
 42 characteristics of a real WSN node platform.

**Table 1.** Empirically obtained path loss exponents ( $n$ ), standard deviations ( $\sigma$  – dB) of the shadowing random variable, and noise floors ( $\overline{P}_n$  – dBm) for six SG environments [1].

Environment	Abbreviation	$n$	$\sigma$	$\overline{P}_n$
Outdoor 500 KV Substation–LOS	OutLOS	2.42	3.12	-93
Outdoor 500 KV Substation–NLOS	OutNLOS	3.51	2.95	-93
Indoor Main Power Room–LOS	InLOS	1.64	3.29	-92
Indoor Main Power Room–NLOS	InNLOS	2.38	2.25	-92
Underground Network Transformer Vault–LOS	UndLOS	1.45	2.45	-88
Underground Network Transformer Vault–NLOS	UndNLOS	3.15	3.19	-88

### 3. System Model

In the following subsections, we present our channel model (in Section 3.1), link-layer energy dissipation model (in Section 3.2), developed optimization method for lifetime maximization (in Section 3.3), and proposed strategies (in Section 3.4), respectively. Throughout this work, we use Tmote Sky mote platforms to construct the WSN which is used for SG applications.

#### 3.1. Wireless Channel Model

We model the wireless channel as a log-normal shadowing channel to calculate the propagation loss. With this respect, the signal-to-noise ratio (i.e.,  $\overline{\gamma}_{ij}(l)$  in dBm) at the receiving node- $j$  due to the transmission from node- $i$  with power level- $l$  can be calculated as

$$\overline{\gamma}_{ij}(l) = \underbrace{\overline{P}_{tx}^{ant}(l) - \overline{PL}_0 + 10n\log_{10}\left(\frac{d_{ij}}{d_0}\right)}_{\overline{P}_{rx,ji}^{ant}(l)} - \overline{X}_\sigma - \overline{P}_n, \quad (1)$$

where  $\overline{P}_{tx}^{ant}(l)$  is the antenna transmit power with transmission power level- $l$  (given in dBm),  $\overline{P}_{rx,ji}^{ant}(l)$  is the reception power (given in dBm),  $\overline{PL}_0 = 55$  dB is the reference path loss value [29],  $n$  is the path loss exponent,  $d_{ij}$  is the distance of a link (in meters),  $d_0$  is the reference distance (in meters),  $\overline{X}_\sigma \sim \mathcal{N}(0, \sigma^2)$  is used to model the shadowing which is a Gaussian random variable with mean zero and variance  $\sigma^2$  (in dB), and  $\overline{P}_n$  is the noise floor.

We consider three different SG environments which are Outdoor 500 KV Substation (i.e., Out), Underground Network Transformer Vault (i.e., Und), and Indoor Main Power Room (i.e., In). We also consider two different propagation characteristics namely as line-of-sight (LOS) and non-line-of-sight (NLOS). Path loss exponents, shadowing variables, and noise floor values are determined with field tests conducted at Georgia Power, Atlanta, GA, USA [1] and are listed in Table 1.

There are eight reported  $P_{tx}^{ant}(l)$  values (i.e., for power levels 3, 7, 11, 15, 19, 23, 27, and 31) available for Chipcon CC2420 radios which are used in Tmote Sky nodes. In order to accurately determine the optimal transmission power levels set, we perform a curve-fitting method to approximately determine all 31 available power levels for CC2420 radios in Figure 1a. Moreover, circuitry transmission power consumption values (i.e.,  $P_{tx}^{cric}(l)$ ) for this radio platform are given in Figure 1b [9].

Tmote Sky platforms use offset quadrature phase shift keying as the modulation scheme. The successful  $L$  bits of data packet reception probability at node- $j$  due to the transmission of node- $i$  with power level- $l$  after

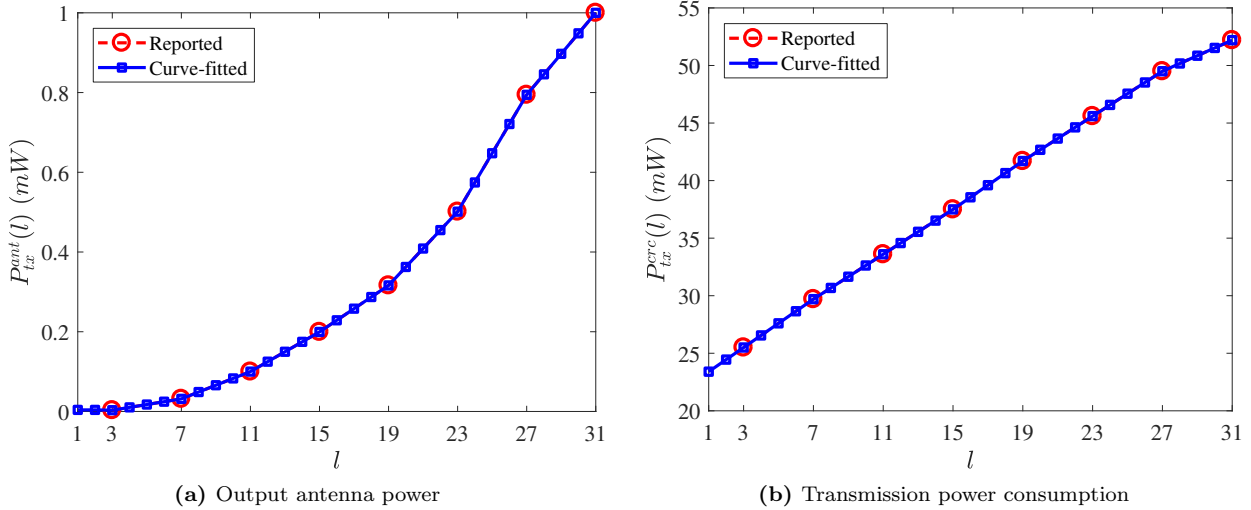


**Figure 1.** Output antenna power ( $P_{tx}^{ant}(l)$  – mW) and power consumption for transmission ( $P_{tx}^{erc}(l)$  – mW) as a function of power levels ( $l$ ) for the CC2420 radio platform.

1 including processing gain costs (i.e.,  $\eta = 16$  [9]), can be calculated as

$$p_{ij}^{s,L}(l) = \left(1 - Q\left(\sqrt{\eta \times \gamma_{ij}(l)}\right)\right)^L, \quad (2)$$

2 where  $\gamma_{ij}(l)$  is the signal-to-noise ratio which is given in ordinary form.  $p_{ij}^{f,L}(l) = 1 - p_{ij}^{s,L}(l)$  shows the  
3 failure reception probability.

### 4 3.2. Link-Layer Energy Dissipation Model

5 We model our link-layer by using a slotted communication scheme such that a single slot consists of durations for  
6  $M_P$ -byte of data packet transmission (i.e.,  $T_{tx}(M_P)$ ),  $M_A$ -byte of acknowledgement (ACK) packet transmission  
7 (i.e.,  $T_{tx}(M_A)$ ), propagation delay (i.e.,  $T_{pd}$ ), and guard times (i.e.,  $2 \times T_{grd}$ ) which are applied at both the  
8 beginning and end of the active slot to prevent synchronization errors [9]. We take  $M_P = 128$  bytes,  $M_A = 12$   
9 bytes, and data rate of Tmote Sky platforms ( $R$ ) as 250 kbps [9]. Thus, we can calculate the active slot time  
10 as:  $T_{slot} = [2 \times T_{grd} + T_{tx}(M_P) + T_{pd} + T_{tx}(M_A)] = 4.78$  ms.

11 A two-way handshaking policy is applied during an active slot to ensure a reliable communication.  
12 A handshaking is considered as successful if both  $M_P$ -byte and  $M_A$ -byte of data and ACK packets are  
13 successfully received at the intended nodes. Hence, we can calculate the probability of the successful handshake  
14 as:  $p_{ij}^{s,HS}(l) = p_{ij}^{s,M_P}(l) \times p_{ji}^{s,M_A}(l)$ . Considering a stop-and-wait ARQ scheme, the expected retransmission rate  
15 is obtained as  $\lambda_{ij}^l = \frac{1}{p_{ij}^{s,HS}(l)}$ .

#### 16 3.2.1. Transmitter Energy Consumption Model

17 Transmission of  $M_P$ -byte of a data packet costs  $P_{tx}^{erc}(l) \times T_{tx}(M_P)$  Joules of energy at the transmitter  
18 node. After transmission of  $M_P$ -byte of a data packet, the transmitter nodes stays in receive/idle mode

1 for  $T_{slot} - T_{tx}(M_P)$  seconds in order to receive an ACK packet. During this period,  $P_{rx}^{crc} \times (T_{slot} - T_{tx}(M_P))$   
 2 Joules of energy is dissipated. In this notation,  $P_{rx}^{crc} = 69$  mW is the power consumption for reception [9].  
 3 Packet processing energy is dissipated only once during a single slot which costs  $E_{PP} = 12.66$   $\mu$ J of energy [9].  
 4 When considering retransmissions with the factor of  $\lambda_{ij}^l$ , overall energy consumption of transmitter node- $i$  can  
 5 be expressed as

$$E_{ij,tx}^l = E_{PP} + \lambda_{ij}^l \times [P_{tx}^{crc}(l) \times T_{tx}(M_P) + P_{rx}^{crc} \times (T_{slot} - T_{tx}(M_P))]. \quad (3)$$

### 6 3.2.2. Receiver Energy Consumption Model

7 The receiver node waits  $T_{slot} - T_{tx}(M_A)$  seconds to receive a data packet from the transmitter node- $i$  which  
 8 costs  $P_{rx}^{crc} \times [T_{slot} - T_{tx}(M_A)]$  Joules of energy. As soon as the data packet is received, node- $j$  uses transmission  
 9 power level- $l$  to transmit an ACK packet back to the node- $i$  in which  $P_{tx}^{crc}(l) \times T_{tx}(M_A)$  Joules of energy is  
 10 dissipated. We define  $\varepsilon$  to denote the amount of energy consumed for data reception and ACK transmission  
 11 during a successful handshake. If the handshaking has failed due to the ACK packet errors in the reverse path,  
 12 we need to repeat the whole handshaking which costs extra energy dissipation with a factor of  $\frac{p_{ij}^{s,MP}(l) \times p_{ji}^{f,MA}(l)}{p_{ij}^{s,HS}(l)}$   
 13 due to the retransmissions. Furthermore, if the data packet is dropped in the forward link, the receiver node  
 14 would stay in receive/idle mode for the whole slot duration in which  $\frac{p_{ij}^{f,MP}(l)}{p_{ij}^{s,HS}(l)} \times [P_{rx}^{crc} \times T_{slot}]$  Joules of energy  
 15 is dissipated while considering retransmissions. Thus, the total energy consumption of the receiving node- $j$  in  
 16 a single slot (with packet processing costs) is obtained as

$$E_{ji,rx}^l = \overbrace{P_{rx}^{crc} [T_{slot} - T_{tx}(M_A)] + [P_{tx}^{crc}(l) \times T_{tx}(M_A)]}^{\varepsilon} + \frac{p_{ij}^{s,MP}(l) p_{ji}^{f,MA}(l)}{p_{ij}^{s,HS}(l)} \varepsilon + \frac{p_{ij}^{f,MP}(l)}{p_{ij}^{s,HS}(l)} (P_{rx}^{crc} \times T_{slot}) + E_{PP}. \quad (4)$$

### 17 3.3. Optimization Model

18 In this part, we model our optimization problem by using MILP technique which maximizes the network lifetime  
 19 (i.e.,  $N$  – in terms of rounds) with limiting the size of the transmission power levels set. The network lifetime is  
 20 defined as the time elapsed until the first node depletes its battery energy [30]. In terms of seconds, the network  
 21 lifetime is calculated as  $N \times T_r$  where  $T_r = 10$  seconds is assumed to be the round duration. We define sets  $V$   
 22 and  $W$  to stand for the set of all nodes (including the base station) and all sensor nodes (excluding the base  
 23 station), respectively. The set  $E$  is used to represent all directed edges (links). The set of transmission power  
 24 levels is defined as  $\mathcal{L}$ . The decision variables of the optimization model is the amount of data packets (size of  
 25 128 bytes) using power level- $l$  traversing from node- $i$  to node- $j$  which is denoted by  $f_{ij}^l$ . The optimization  
 26 model with its constraints is given in Figure 2.

27 In (5) incoming flows, generated flows at each round (i.e.,  $N \times s_i$ ), and outgoing flows are balanced  
 28 at each sensor node- $i$ . Total active time for sensor node- $i$  (i.e.,  $T_{act}^i$ ) consist of durations for transmission,  
 29 reception, and acquiring data including retransmissions which is calculated in (6). Note that  $T_{DA} = 5$  ms is the  
 30 time to acquire a data packet which is dissipated once per round [9]. In (7), energy required for transmission,  
 31 reception, sleep, and data acquisition at each sensor node- $i$  limited to initial battery of each node (i.e.,  $\varrho =$   
 32 25 KJ). In this constraint,  $E_{DA} = 57$   $\mu$ J is the energy consumed for data acquisition and  $P_{slp} = 3$   $\mu$ W is

Maximize  $N \times T_r$   
 Subject to:

$$\sum_{l \in \mathcal{L}} \sum_{j \in V} f_{ij}^l - \sum_{l \in \mathcal{L}} \sum_{j \in W} f_{ji}^l = N \times s_i, \forall i \in W \quad (5)$$

$$T_{act}^i = T_{slot} \sum_{l \in \mathcal{L}} \left( \sum_{j \in V} \lambda_{ij}^l f_{ij}^l + \sum_{j \in W} \lambda_{ji}^l f_{ji}^l \right) + N \times T_{DA}, \forall i \in W \quad (6)$$

$$\sum_{l \in \mathcal{L}} \sum_{j \in V} E_{ij,tx}^l f_{ij}^l + P_{slp} \times (N \times T_r - T_{act}^i) + \sum_{l \in \mathcal{L}} \sum_{j \in W} E_{ji,rx}^l f_{ji}^l + N \times E_{DA} \leq \varrho, \forall i \in W \quad (7)$$

$$T_{slot} \sum_{l \in \mathcal{L}} \left( \sum_{j \in V} \lambda_{ij}^l f_{ij}^l + \sum_{j \in W} \lambda_{ji}^l f_{ji}^l + \sum_{(j,n) \in E} \lambda_{jn}^l f_{jn}^l I_{jn}^{i,l} \right) \leq N \times T_r, \forall i \in V \quad (8)$$

$$\sum_{(i,j) \in E} f_{ij}^l \leq \mathcal{M} \times b_l, \forall l \in \mathcal{L} \quad (9)$$

$$\sum_{l \in \mathcal{L}} b_l \leq \beta \quad (10)$$

$$f_{ij}^l \geq 0, \forall l \in \mathcal{L}, \forall (i,j) \in E \quad (11)$$

$$b_l \in \{0, 1\}, \forall l \in \mathcal{L} \quad (12)$$

**Figure 2.** The optimization model to maximize network lifetime with limiting the size of the transmission power levels set.

1 the sleep power [9]. (8) is used for each node- $i$  to limit the aggregated duration of incoming, outgoing, and  
 2 interfering flows to the total network lifetime in seconds. Interference function at node- $i$  (i.e.,  $I_{jn}^{i,l}$ ) takes the  
 3 value of 1 if node- $i$  can hear the transmission between node- $j$  and node- $n$  (i.e.,  $\overline{P_{rx,ji}^{ant,l}} \geq \overline{P_{sns}}$  or  $\overline{P_{rx,ni}^{ant,l}} \geq \overline{P_{sns}}$   
 4 where  $\overline{P_{sns}} = -94$  dBm is the nominal receiver sensitivity for the Tmote Sky mote platforms). We define the  
 5 binary decision variable  $b_l$  to denote that whether the transmission power level- $l$  is used (i.e.,  $b_l = 1$ ) or not  
 6 (i.e.,  $b_l = 0$ ). By using  $b_l$ , in (9), we prohibit the flows using power level- $l$  within the network if  $b_l = 0$ . In  
 7 (10) the set size of the transmission power levels is limited to  $\beta$  (which is a constant). Finally, (11) and (12)  
 8 show the boundaries of the decision variables used in the optimization model.

### 9 3.4. Proposed Strategies

10 In this part, we present the principles of our proposed strategies that are used to determine the most used (in  
 11 Section 3.4.1) and optimal transmission power levels (in Section 3.4.2) sets for lifetime maximization in WSN  
 12 based SG applications. Note that both methodologies use the base optimization framework given in Figure 2.

#### 13 3.4.1. Histogram Based Power Levels Decision (HB-PLD) Strategy

14 In HB-PLD strategy, we first determine the most used transmission power levels for a given WSN topology and  
 15 SG environment without enforcing any constraints on the set size of the transmission power levels (hence all

available power levels can freely be utilized). For this purpose, we solve the optimization problem in Figure 2 without constraints given in (9), (10), and (12). According to the optimal flows obtained by solving the optimization model (i.e.,  $f_{ij}^l$ ), a histogram of power levels utilization is prepared. By using the prepared histogram, most utilized power levels are sorted in descending order and corresponding  $b_l$  values are marked as 1 (note that the binary variable,  $b_l$ , is treated as a parameter). In order to investigate the impact of most used transmission power levels set size on the network lifetime, we re-active the constraints in (9), (10), and (12). Then we set  $\beta$  to 16 (only the most used 16 power levels can be utilized) and set the parameter  $b_l$  as 1 for the most used 16 power levels to observe the changes occurred in the network lifetime. This process continues as  $\beta$  is lowered to 8, 4, 2, and 1.

### 3.4.2. Optimization Based Power Levels Decision (OB-PLD) Strategy

In OB-PLD strategy, determination of optimal transmission power levels is performed by the optimization model given in Figure 2 instead of a histogram based approach as stated in the previous part. Different from HB-PLD strategy,  $b_l$  is considered as a binary variable and all constraints presented in Figure 2 are active.

The optimization model given in Figure 2 decides whether the power level- $l$  is used or not by using the binary variable,  $b_l$ . For example, if  $b_1 = 1$ , then power level-1 is utilized and vice versa. If the power level- $l$  cannot be utilized (i.e.,  $b_l = 0$ ), according to the constraint (9),  $\sum_{(i,j) \in E} f_{ij}^l \leq 0$ . Since  $f_{ij}^l \geq 0$  by (11), there will be no data traffic traversing in the network by using power level- $l$  (i.e.,  $f_{ij}^l$  values are forced to be equal to 0  $\forall (i,j) \in E$ ). On the other hand, if the power level- $l$  is used, then  $\sum_{(i,j) \in E} f_{ij}^l \leq \mathcal{M}$  according to (9). This inequality states that the amount of data packets using power level- $l$  flowing through the all links are bounded to a very large number,  $\mathcal{M}$ . In this way,  $f_{ij}^l$  values can take positive values. By summing all  $b_l$  values, the set size of the transmission power levels are determined since  $b_l$  values can only be either 0 or 1. In OB-PLD strategy, the optimization model given in Figure 2 aims to determine the optimal values of  $b_l$  that maximize the network lifetime while satisfying the set size of the transmission power levels constraint (i.e.,  $\sum_{l \in \mathcal{L}} b_l \leq \beta$ ). In this notation,  $\beta$  is the upper bound of the set size of the transmission power levels. For example, if  $\beta = 8$  (i.e., at most 8 power levels can be utilized), then at most eight  $b_l$  values can be 1. Indeed, the optimization model determines which power level to be used for lifetime maximization by setting appropriate  $b_l$  values to be 1. As in the HB-PLD strategy, we change  $\beta$  values as 31, 16, 8, 4, 2, and 1, respectively in order to characterize the effects of  $\beta$  on network lifetime.

## 4. Analysis

In this part we perform the analysis to determine most used and optimal transmission power levels set size and investigate their impacts on network lifetime. The WSN topology is modeled as a disk with radius  $R_{net}$  and 39 sensor nodes are randomly distributed within the disk obeying a uniform distribution. The base station is centered at the disk.

We choose three  $R_{net}$  values to model a good, a mediocre, and a bad channel condition for each SG propagation environment such that average successful handshaking probabilities of all links and power levels (i.e.,  $E[p_{HS}^s] = \frac{\sum_{l \in \mathcal{L}} \sum_{(i,j) \in E} P_{ij}^{s,HS}(l)}{|E| \times |\mathcal{L}|}$ ) are approximately 0.80, 0.50, and 0.25. The chosen  $R_{net}$  values are reported in Table 2. The wireless channel model (Section 3.1) and the link-layer energy dissipation model

**Table 2.** Network radii (i.e.,  $R_{net}$ ) in meters and corresponding average successful handshake probabilities (i.e.,  $E[p_{HS}^s]$ ) for six SG environments.

$E[p_{HS}^s]$	Network radii for six SG environments (in meters)					
	OutLOS	OutNLOS	InLOS	InNLOS	UndLOS	UndNLOS
0.80	10	5	10	5	25	5
0.50	25	10	50	20	200	10
0.25	50	20	120	30	400	20

(Section 3.2) are developed in MATLAB <sup>2</sup>. Proposed strategies (Section 3.4) are modeled and solved with General Algebraic Modeling System (GAMS) <sup>3</sup>.

In this work, a stable communication channel is employed on each link such that path loss values do not change over network lifetime. In the following figures, we present the average values of 50 independent runs where at each run both topology and path loss values for each link are regenerated. Since path loss values vary greatly in each scenario, variations in the channel conditions have already been considered in our work. Nevertheless, in [31] it is shown that channel conditions for WSNs can be accurately estimated with very low overhead. We assume that the base station has the knowledge of topology as in [8]. Since the base station in a typical WSN has higher computational capacity and larger battery power than ordinary nodes, path loss calculations and other necessary decision making actions related to the optimization (data flow planning via optimization, routing, etc.) are performed at the base station in a centralized manner.

We present the cumulative percentage of power levels utilization which maximizes the network lifetime when there are no restrictions on the set size of transmission power levels (i.e.,  $\beta = 31$ ) for OutLOS in Figure 3a, InLOS in Figure 3b, UndLOS in Figure 3c, OutNLOS in Figure 3d, InNLOS in Figure 3e, and UndNLOS in Figure 3f, respectively. In each subfigure, three  $R_{net}$  values are used (see Table 2) for each environment. Each subfigure is obtained by solving the HB-PLD strategy and creating a histogram of the power level utilization by inspecting the  $l$  index of  $f_{ij}^l$  values for 50 different network topologies. It is also important to note that HB-PLD and OB-PLD strategies yield exactly the same results when there are no restrictions on the cardinality of transmission power levels set. The reason behind this fact is the constraints given in (9), (10), and (12) in OB-PLD strategy such that these constraints have already been satisfied when  $\beta = 31$ . Thus, these constraints can be classified as redundant constraints and consecutively OB-PLD strategy converges to HB-PLD strategy.

Regardless of the environment, we see that for a dense network (i.e., small  $R_{net}$  values) at least 88% of the links utilize power levels less than or equal to 8. As the network size increases, the network gets sparser hence the utilization percentage of higher power levels increases to reduce the packet errors. When we consider a moderately dense network (i.e., mediocre  $R_{net}$  values), the utilization of power levels greatly varies such that we observe that at least 90% of the links utilize transmission power levels less than 26. When the network density is very low (i.e., high  $R_{net}$  values), at least 78% of the links utilize power levels except for the highest power level (i.e.,  $l = 31$ ). This means that at most 22% of the links utilize the highest transmission power level. According to these data, we can infer that it is important to carefully choose transmission power levels according

<sup>2</sup><https://www.mathworks.com/products/matlab.html>

<sup>3</sup><https://www.gams.com/>

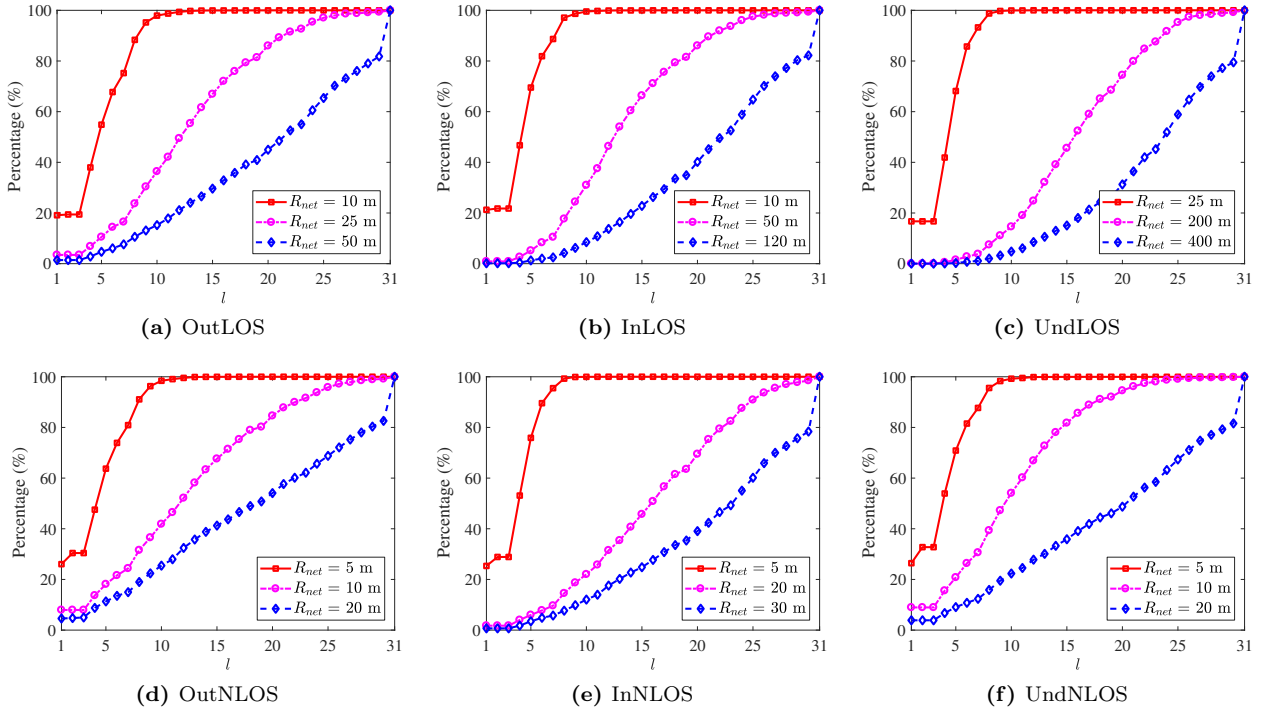


**Figure 3.** Cumulative percentage of power level utilization for HB-PLD strategy considering six SG environments with three  $R_{net}$  values for each environment when  $\beta = 31$ .

1 to the network conditions for network lifetime maximization. The reported eight power levels for Tmote Sky  
 2 motes using Chipcon CC2420 radios (i.e.,  $l = 3, 7, 11, 15, 19, 23, 27,$  and  $31$ ) may lead misleading results for  
 3 accurately estimating the network lifetime. Note that for denser networks low power levels (e.g., power levels 3  
 4 to 7) are likely to be used, while for sparse networks high power levels (e.g., power levels 30 and 31) are tended  
 5 to be utilized. Overall, these results indicate that utilization of all available power levels is unnecessary.

6 We present network lifetimes of the proposed strategies for OutLOS in Figure 4a, InLOS in Figure 4b,  
 7 UndLOS in Figure 4c, OutNLOS in Figure 4d, InNLOS in Figure 4e, and UndNLOS in Figure 4f, respectively.  
 8 In each subplot, one SG environment is considered and six curves are presented which correspond to the results  
 9 of HB-PLD and OB-PLD strategies with three  $R_{net}$  values for each strategy. In each curve, normalized lifetimes  
 10 are presented with respect to the cardinality of the optimum transmission power levels set (i.e.,  $\beta$ ) in order to  
 11 investigate the relative impact of limiting the size of transmission power levels set on network lifetime. Note  
 12 that  $\beta$  values are given in descending order for the sake of visually. Normalized lifetimes are obtained by diving  
 13 each lifetime value obtained with a specific  $\beta$  by the lifetime which is obtained without any constraints on the  
 14 size of the transmission power levels set (i.e.,  $\beta = 31$ ).

15 For both HB-PLD and OB-PLD strategies normalized lifetimes decrease as  $\beta$  decreases. Normalized  
 16 lifetimes can be as low as 0.11 and as high as 0.62 for HB-PLD strategy (OutNLOS environment with  $\beta = 1$   
 17 and  $R_{net} = 10$  m & 20 m, respectively). As shown in Figure 3d, when  $R_{net} = 10$  m, the most used power level  
 18 is the minimum transmission power level (i.e.,  $l = 1$ ) such that around 8% of the links utilize this power level.  
 19 Hence, when  $\beta = 1$ , HB-PLD strategy enforces all links to utilize the minimum transmission power level. Since

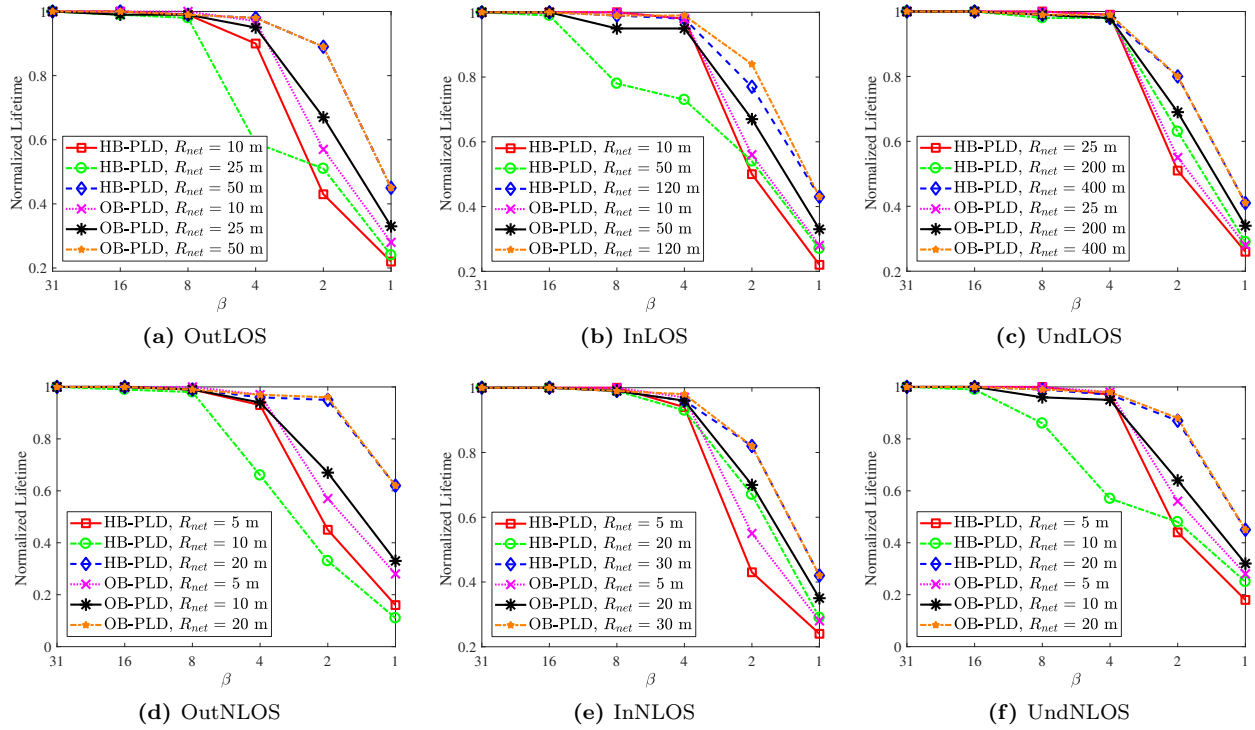


**Figure 4.** Normalized network lifetimes for HB-PLD and OB-PLD strategies as a function of  $\beta$  for six SG environments and three  $R_{net}$  values for each environment.

1 the utilization of minimum transmission power level leads more packet errors that incurs extra retransmissions,  
 2 more energy is consumed which reduces the network lifetime drastically. On the other hand, as the network gets  
 3 sparser (i.e.,  $R_{net} = 20$  m), the most utilized power level is the maximum transmission power level which is used  
 4 around 17% of the links. In this case,  $\beta = 1$  constraint employs all links to utilize power level 31 which would  
 5 reduce the packet errors, thus extra energy dissipation due to the retransmissions are mostly mitigated yielding  
 6 less drops in maximum lifetime. Similar interpretations are also valid for other SG environments. Setting the  
 7 set size of transmission power levels 16 would lead at most 1% drop in maximum network lifetime for HB-PLD  
 8 strategy. Nevertheless, for  $\beta \leq 8$  sparser networks have the highest normalized lifetime values. This result may  
 9 be explained by the fact that the variation of power levels used for sparse networks is less since higher power  
 10 levels are preferred for reliable communications when the network size is large.

11 As stated before, HB-PLD and OB-PLD lifetimes are exactly the same when all available transmission  
 12 power levels can be utilized. HB-PLD and OB-PLD lifetimes are also same when  $\beta = 1$  and the network is  
 13 sparse due to the fact of utilization of highest power level as stated in the previous paragraph. When the size of  
 14 the power levels set is halved (i.e.,  $\beta = 16$ ), we observe that OB-PLD lifetimes are at most 0.68% higher than  
 15 HB-PLD lifetimes. As  $\beta$  decreases, OB-PLD strategy yields better lifetimes. For example, OB-PLD lifetimes  
 16 are at most 22.05%, 68.67%, 101.85%, and 199.53% higher than HB-PLD lifetimes for  $\beta = 8, 4, 2,$  and 1,  
 17 respectively. These results are related to suboptimal behavior of HB-PLD strategy. For OutNLOS environment  
 18 with  $R_{net} = 10$  m, we stated that the most common power level utilized is the minimum transmission power  
 19 level. When  $\beta = 1$ , HB-PLD strategy enforces links to use  $l = 1$ . However, OB-PLD strategy tries to utilize

the optimum power level for this configuration which is obtained as the highest transmission power level. This is the reason that OB-PLD lifetimes can be 199.53% higher than the HB-PLD lifetimes. Nevertheless, normalized lifetimes for OB-PLD strategy can be as low as 0.28 and as high as 0.62. If the set size of transmission power levels is chosen as 4, the drop in maximum lifetime is observed between 1% and 6%.

The solution times for OB-PLD strategy are generally higher than the solution times for HB-PLD strategy due to the  $b_l$ . Note that, in HB-PLD strategy  $b_l$  is defined as a parameter. On the other hand, in OB-PLD strategy  $b_l$  is a binary variable which naturally increases the solution times for the OB-PLD strategy. Moreover, solution times for OB-PLD strategy greatly increases as  $\beta$  decreases since the constraint defined in (10) becomes tighter as  $\beta$  decreases. The computations are performed on a computer with 2.30 GHz Intel Core i5-6200U processor and 8 GB of RAM. Our analysis reveals that solution times are in the interval 5.53–29.30 seconds and 6.86–40.48 seconds for HB-PLD and OB-PLD strategies, respectively.

## 5. Conclusion

In this work, two strategies are proposed (i.e., HB-PLD and OB-PLD) to determine the most used and optimal transmission power levels sets for lifetime maximization in WSN based SGs. Proposed strategies are formulated by using an MILP framework which is built on top a detailed link-layer energy dissipation model with an empirically verified channel model. Quantitative analysis is performed on a disk shaped WSN such that nodes are randomly deployed for six SG environments.

Our main conclusions are enumerated as follows:

1. The set size of transmission power levels is small for either dense or sparse networks. For dense/sparse networks lower/higher transmission power levels are utilized. On the other hand, if a network is moderately dense, the set size of transmission power levels gets larger due to the variations of power level utilization on links.
2. Utilization of all available power levels is unnecessary regardless of the network topology and the SG environment. Our analysis shows that using only 16 power levels out of 31 power levels would lead a maximum lifetime drop at most 1%.
3. Although the implementation of HB-PLD strategy is relatively easy (due to the treatment of the binary variable as a parameter), determination of transmission power levels set size by using this strategy can greatly underestimate the network lifetime when compared to the OB-PLD strategy if the set size of transmission power levels is planned to be small. Indeed, OB-PLD lifetimes are at most 2 times greater than HB-PLD strategy if a single global power level is planned to be used throughout the all links in the network.
4. HB-PLD strategy can be used with insignificant lifetime deterioration (at most 1% drop) if the half of the available power levels are used. However, as the set size of transmission power levels is lessened, OB-PLD strategy should be employed for lifetime maximization.
5. Using only 4 transmission power levels in OB-PLD strategy results in maximum lifetime drop between 1% and 6% regardless of the network size and channel conditions. For this set size, the drop in maximum network lifetime would be at most 43% if HB-PLD strategy is employed. This result is useful for designing distributed protocols focused on transmission power control where the burden of utilization of all power levels can greatly be eased by using our proposed solution if the network conditions are unknown.

## References

- [1] Güngör VÇ, Lu B, Hancke GP. Opportunities and challenges of wireless sensor networks in smart grid. *IEEE T Ind Electron* 2010; 57: 3557–3564.
- [2] Parikh PP, Kanabar MG, Sidhu TS. Opportunities and challenges of wireless communication technologies for smart grid applications. In: *IEEE PES General Meeting*; 25–29 July 2010; Providence, RI, USA: IEEE. pp. 1–7.
- [3] Şahin D, Güngör VÇ, Koçak T, Tuna G. Quality-of-service differentiation in single-path and multi-path routing for wireless sensor network-based smart grid applications. *Ad Hoc Netw* 2014; 22: 43–60.
- [4] Saputro N, Akkaya K, Uludağ S. A survey of routing protocols for smart grid communications. *Comput Netw* 2012; 56: 2742–2771.
- [5] Gao J, Xiao Y, Liu J, Liang W, Chen CLP. A survey of communication/networking in smart grids. *Future Gener Comput Syst* 2012; 28: 391–404.
- [6] Fadel E, Güngör VÇ, Nassef L, Akkari N, Malik MGA, Almasri S, Akyıldız IF. A survey on wireless sensor networks for smart grid. *Comput Commun* 2015; 71: 22–33.
- [7] Tantur Ç, Yıldız HU, Kurt S, Tavlı B. Optimal transmission power level sets for lifetime maximization in wireless sensor networks. In: *IEEE SENSORS*; 30 October–3 November 2016; Orlando, FL, USA: IEEE. pp. 1–3.
- [8] Yıldız HU, Tavlı B, Yanıkömeroğlu H. Transmission power control for link-level handshaking in wireless sensor networks. *IEEE Sens J* 2016; 16: 561–576.
- [9] Kurt S, Yıldız HU, Yiğit M, Tavlı B, Güngör VÇ. Packet size optimization in wireless sensor networks for smart grid applications. *IEEE T Ind Electron* 2017; 64: 2392–2401.
- [10] Hossain AZME, Sarker JH. On throughput performance of single and multichannel S-ALOHA with exponential backoff retransmission schemes for packet transmissions in multiple power levels. In: *IEEE International Conference on Personal Wireless Communications (Cat. No. 97TH8338)*; 17–19 December 1997; Mumbai, India: IEEE. pp. 152–156.
- [11] Liu TY, Scholtz RA. An optimal link power set for a mobile communication network with directive/adaptive antennas. In: *MILCOM 97 Proceedings*; 3–5 November 1997; Monterey, CA, USA: IEEE. pp. 782–786.
- [12] Lin L, Yates RD, Spasojevic, P. Adaptive transmission with discrete code rates and power levels. *IEEE T Commun* 2003; 51: 2115–2125.
- [13] Karmokar AK, Djonin DV, Bhargava VK. Delay constrained rate and power adaptation over correlated fading channels. In: *IEEE Global Telecommunications Conference (GLOBECOM)*; 29 November–3 December 2004; Dallas, TX, USA: IEEE. pp. 3448–3453.
- [14] Khoshnevis B, Khalaj BH. On a decentralized deterministic transmission power level selection algorithm in large aloha networks under saturation. In: *IEEE International Conference on Communications*; 11–15 June 2006; İstanbul, Turkey: IEEE. pp. 5732–5737.
- [15] Gjendemsjo A, Oien GE, Orten P. Optimal discrete-level power control for adaptive coded modulation schemes with capacity-approaching component codes. In: *IEEE International Conference on Communications*; 11–15 June 2006; İstanbul, Turkey: IEEE. pp. 5047–5052.
- [16] Srinivasa S, Jafar SA. Soft sensing and optimal power control for cognitive radio. *IEEE T Wirel Commun* 2010; 9: 3638–3649.
- [17] Noack A, Bok PB, Kruck S. Evaluating the impact of transmission power on QoS in wireless mesh networks. In: *International Conference on Computer Communications and Networks (ICCCN)*; 31 July–4 August 2011; Maui, HI, USA: IEEE. pp. 1–6.
- [18] Su W, Lee S, Pados DA, Matyjas JD. Optimal power assignment for minimizing the average total transmission power in hybrid-ARQ rayleigh fading links. *IEEE T Commun* 2011; 59: 1867–1877.
- [19] Zou M, Chan S, Vu HL, Ping L. Throughput improvement of 802.11 networks via randomization of transmission power levels. *IEEE T Veh Technol* 2016; 65: 2703–2714.

- 1 [20] Nar PC, Çayırıcı E. PCSMAC: a power controlled sensor-MAC protocol for wireless sensor networks. In: Proceed-  
2 ings of the Second European Workshop on Wireless Sensor Networks; 2–2 February 2005; İstanbul, Turkey: IEEE.  
3 pp. 81–92.
- 4 [21] Galluccio L, Leonardi A, Morabito G, Palazzo S. On the convenience of turning off the radio interface and  
5 using multiple transmission power levels in sensor networks applying geographical forwarding. In: International  
6 Symposium on Wireless Communication Systems; 6–8 September 2006; Valencia, Spain: IEEE. pp. 88–92.
- 7 [22] Natarajan A, Silva B, Yap KK, Motani M. Link layer behavior of body area networks at 2.4 GHz. In: International  
8 Conference on Mobile Computing and Networking; 20–25 September 2009; Beijing, China: ACM. pp. 241–252.
- 9 [23] Lee W, Choi M, Kim N. Experimental link channel characteristics in wireless body sensor systems. In: The  
10 International Conference on Information Network; 1–3 February 2012; Bali, Indonesia: IEEE. pp. 374–378.
- 11 [24] Zogovic N, Dimic G, Bajic D. Packet length and transmission power adaptation for energy-efficiency in low-  
12 power wireless communications. In: International Conference on Telecommunication in Modern Satellite Cable  
13 and Broadcasting Services (TELSIKS); 5–8 October 2011; Nis, Serbia: IEEE. pp. 497–500.
- 14 [25] Farayev B, Sadi Y, Ergen SÇ. Optimal power control and rate adaptation for ultra-reliable M2M control applications.  
15 In: IEEE Globecom Workshops (GC Wkshps); 6–10 December 2015; San Diego, CA, USA: IEEE. pp. 1–6.
- 16 [26] Jouhari M, Ibrahim K, Benattou M. Topology control through depth adjustment and transmission power control  
17 for UWSN routing protocols. In: International Conference on Wireless Networks and Mobile Communications  
18 (WINCOM); 20–23 October 2015; Marrakech, Morocco: IEEE. pp. 1–5.
- 19 [27] Liu CH, Rong B, Cui S. Optimal discrete power control in poisson-clustered ad hoc networks. *IEEE T Wirel*  
20 *Commun* 2015; 14: 138–151.
- 21 [28] Sisodiya N, Shetty DP. Total power minimization using dual power assignment in wireless sensor networks. In:  
22 International Conference on Information Technology (ICIT); 21–23 December 2015; Bhubaneswar, India: IEEE.  
23 pp. 26–30.
- 24 [29] Zuniga M, Krishnamachari B. Analyzing the transitional region in low power wireless links. In: IEEE Communi-  
25 cations Society Conference on Sensor and Ad Hoc Communications and Networks (SECON); 4–7 October 2004;  
26 Santa Clara, CA, USA: IEEE. pp. 517–526.
- 27 [30] Yetgin H, Cheung KTK, El-Hajjar M, Hanzo LH. A survey of network lifetime maximization techniques in wireless  
28 sensor networks. *IEEE Commun Surv Tut* 2017; 19: 828–854.
- 29 [31] Lin S, Zhang J, Zhou G, Gu L, He T, Stankovic JA. ATPC: adaptive transmission power control for wireless sensor  
30 networks. In: International Conference on Embedded Networked Sensor Systems (SenSys); 31 October–3 November  
31 2006; Boulder, CO, USA: ACM. pp. 223–236.